ACS Chemical Neuroscience pubs.acs.org/acschemicalneuroscience Article

Inhibition of Aβ42 Peptide Aggregation by a Binuclear Ruthenium(II)−Platinum(II) Complex: Potential for Multimetal Organometallics as Anti-amyloid Agents

Amit Kumar,[†] LaMaryet Moody,[†] Jason F. Olaivar,[†] Nerissa A. Lewis,[†] Rahul L. Khade,[†] Alvin A. Holder,[†] Yong Zhang,[†,‡] and Vijayaraghavan Rangachari*[,†]

[†]Department of Chemistry and Biochemistry, University of Southern Mississippi, 118 College Dr No. 5043, Hattiesburg, Mississippi 39406, and [‡]Department of Chemistry, Chemical Biology, and Biomedical Engineering, Stevens Institute of Technology, Castle Point on Hudson, Hoboken, New Jersey 07030

Abstract

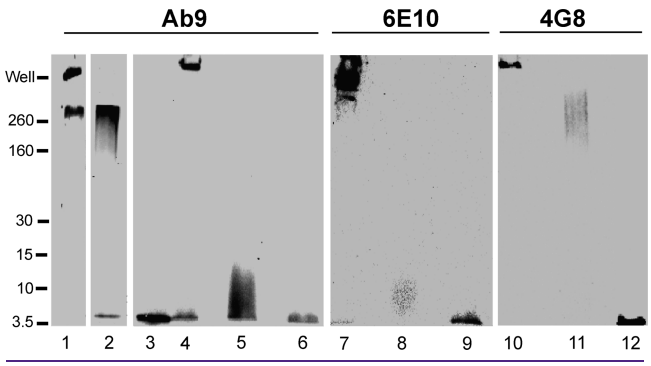

Design of inhibitors for amyloid-β (Aβ) peptide aggregation has been widely investigated over the years toward developing viable therapeutic agents for Alzheimer's disease (AD). The biggest challenge seems to be inhibiting Aβ aggregation at the early stages possibly at the monomeric level, because oligomers are known to be neurotoxic. In this regard, exploiting the metal-chelating property of Aβ to generate molecules that can overcome this impediment presents some promise. Recently, one such metal complex containing Pt^{II} ([Pt(BPS)Cl_2]) was reported to effectively inhibit Aβ42 aggregation and toxicity (Barnham, et al. (2008) *Proc. Natl. Acad. Sci. U.S.A. 105*, 6813). This complex was able bind to Aβ42 at the N-terminal part of the peptide and triggered a conformational change resulting in effective inhibition. In the current report, we have generated a mixed-binuclear metal complex containing Pt^{II} and Ru^{II} metal centers that inhibited Aβ42 aggregation at an early stage and seemed to have different modes of interaction than the previously reported Pt^{II} complex, suggesting an important role of the second metal center. This 'proof-of-concept' compound will help in developing more effective molecules against Aβ aggregation by modifying the two metal centers as well as their bridging ligands, which will open doors to new rationale for Aβ inhibition.

Keywords: Amyloid, aggregation, inhibitor, platinum(II), ruthenium(II), organometallics, cisplatin, and intercalation

Alzheimer's disease (AD) is a progressive neurodegenerative disorder that leads to cognitive decline and dementia in the elderly. AD is one of the most common neurological disorders and more than 5 million people are affected in the United States alone. This number is expected to quadruple in the next few decades if no breakthrough is made toward drug discovery for combating AD (*2*). Brains of patients with AD contain large deposits of senile plaques composed mainly of 40- and 42-residue peptides called amyloid-β (Aβ) peptides. Aβ peptides undergo aggregation to form large extracellular fibrillar aggregates that deposit as plaques. Considerable evidence suggests that cognitive decline and dementia in AD patients arise from the formation of various aggregated forms of Aβ, including oligomers, protofibrils, and fibrils, and recent reports propose that low molecular weight soluble oligomers of Aβ are the primary neurotoxic agents responsible for memory deficits (*3*−*6*). Therefore, there is significant interest in developing inhibitors of Aβ aggregation toward meaningful therapeutic agents for the treatment of AD. Many rationally designed molecules have emerged as a consequence including β-sheet breakers (*7*, *8*), N-methylated peptides (*9*), and ΔAla-containing peptides (*10*), to name a few. In addition to these, natural products such as curcumin, vitamin A, and others containing polyhydroxy phenols have been found to be effective inhibitors and in mitigating amyloid toxicity in transgenic mouse models (*11*−*13*).

The interaction of transition metals with Aβ peptide has been well characterized and is thought to play an important role in AD. Transition metal cations such as Cu^{2+}, Zn^{2+}, and Fe^{3+} are enriched in amyloid plaques observed in AD brains (*14*−*16*) and are known to possess high affinity of binding for Aβ and mediate the process of aggregation *in vitro* (*17*). Zn^{2+} at submicromolar concentrations was able to precipitate Aβ rapidly, while Cu^{2+} and Fe^{3+} induced marked Aβ aggregation under

Received Date: May 7, 2010
Accepted Date: July 27, 2010
Published on Web Date: August 23, 2010

DOI: 10.1021/cn100046m | *ACS Chem. Neurosci.* (2010), *1*, 691–701

mildly acidic conditions (*18*). Moreover, nanomolar concentrations of these metals in buffers were able to induce nucleation during Aβ aggregation that lead to increased rates of aggregation (*19*). The interactions between Aβ and metal ions extensively studied; however, affinity of metals toward Aβ vary to a large extent. Affinity constants (K_d) for Zn^{2+} binding to Aβ40 lie between 100 nM (*18*) and 300 μM (*17*), and those for Cu^{2+} lie between 0.1 nM (*19*) and 10 μM. Nevertheless, Aβ−metal interactions are well characterized and binding is known to occur at the N-terminus and histidines at the 6th and 13th or 14th position in Aβ (*20*). More importantly, metal ion coordination can be utilized to engineer specificity of binding to regulate amyloid toxicity (*21*).

Recently, Barnham and colleagues reported the use of Pt^{II} complexes against Aβ42 aggregation and toxicity (*1*). Pt^{II} complexes have been used as drugs for cancer treatment for a number of years (*22*−*24*). One such example is *cisplatin* (*cis*-[$Pt(NH_3)_2Cl_2$]), which is a well-known interchelator of DNA used in chemotherapy. As far as we know, the report by Barnham et al. (*1*) is the first attempt to use metal complexes against Aβ aggregation that takes advantage of inherent metal binding ability of Aβ, which has opened interesting new avenues for inhibitor designs. They reported that several metal complexes containing a Pt^{II} metal center inhibited Aβ42 aggregation in vitro and mitigated Aβ neurotoxicity in primary mouse neuronal cell culture. Among the complexes investigated, (4,7-diphenyl-[1,10]phenanthroline disulfonate)Cl_2 (Pt-1; Figure 1A) seemed to be the most effective in inhibiting Aβ aggregation. The Pt^{II} metal center in the complex was shown to at least bind to histidine residues. This suggested that the phenanthroline ligand in Pt-1 was able to confer specificity as well as increase its binding affinity to Aβ. Although phenanthroline, like many polyaromatic compounds, has a weak affinity for Aβ, the binding of Pt^{II} increased the overall affinity for Aβ resulting in effective inhibition of aggregation. This report has opened an opportunity for rational design of inhibitors by exploiting the well-established metal binding capability of Aβ peptide. One rationale would be to keep the metal binding center as an "anchor" and generate appropriate ligands around it such that the secondary interactions with Aβ are optimized to alter the latter's conformation leading to effective inhibition.

In this context, multimetal complexes can play unique roles. It is interesting to note that recent studies indicate the DNA binding capabilities of the Pt^{II}-containing complexes with the *cis*dichloro moiety, [(L)$Pt^{II}Cl_2$] (L denotes ligand), can be enhanced by incorporating another metal moiety through bridging ligands (*25*, *26*). Many such complexes containing Pt^{II} and Ru^{II} centers have been investigated by Brewer and co-workers (*27*−*29*). A wide assortment of polyazine bridging ligands exists, and many Ru^{II} complexes of these ligands have been investigated. Ruthenium complexes of the 2,3-bis(2-pyridyl)benzoquinoxaline (dpb) bridging ligand have been shown by Murphy et al (*30*) to interact with DNA, who postulated that the interaction occurs via intercalation of the ligand. These observations prompted us to evaluate the rationale of using Pt^{II}, Ru^{II} containing complexes to further improve Aβ inhibition. Therefore, in this report, we designed a binuclear complex containing Pt^{II} and Ru^{II} metal centers ([$(bpy)_2Ru^{II}(dpp)Pt^{II}Cl_2]Cl_2$; Figure 1B) and analyzed its inhibitory capability toward Aβ aggregation as compared with the previously reported Pt-1. We observed that although the overall inhibition was comparable between the two complexes, there were distinct differences between their modes of interaction and possibly mechanisms. The data have encouraged us to explore more avenues in designing new multimetal complexes to improve Aβ inhibition.

Results

Rationale for Design

We designed our compound containing two metal centers, viz Pt^{II} and Ru^{II}, named PtRu-1 ([$(bpy)_2Ru^{II}$-$(dpp)Pt^{II}Cl_2]Cl_2$; Figure 1B) based on the compound Pt-1 (Figure 1A) that has been previously reported to effectively inhibit Aβ aggregation (*1*). We have used Pt-1 as our positive control in our current study. A previous report suggested that the presence of phenylsulfonate groups within Pt-1 seemed to improve the ability of the compound to inhibit Aβ aggregation (*1*). Hence, the authors hypothesized that the introduction of phenylsulfonate groups might be involved in favorable secondary hydrophobic interactions within the Aβ peptide. Bearing this in mind, we designed PtRu-1 by retaining the platinum binding site and introducing a second metal center containing Ru^{II} via a bridging ligand and hydrophobic bipyridyl ligand for Ru^{II} center for two important reasons: (i) since recent studies indicate that the DNA binding capabilities of the Pt^{II}-containing complexes, [(L)$Pt^{II}Cl_2$], could be enhanced by incorporating another metal moiety through bridging ligands (*25*, *26*), we reasoned that similar modification to the reported Pt-1 might result in increased inhibition capability, and (ii) the bipyridyl ligands (similar to polyaromatic compounds) coordinating to Ru^{II} will generate a large hydrophobic surface that may enhance the ability of the compound to interact with similar surfaces present in Aβ peptide. As a consequence, we expected both to enhance the binding ability of the Pt^{II} metal center to Aβ42 and to stabilize other secondary interactions, making the molecule effective for Aβ42 inhibition.

DOI: 10.1021/cn100046m | *ACS Chem. Neurosci.* (2010), *1*, 691–701

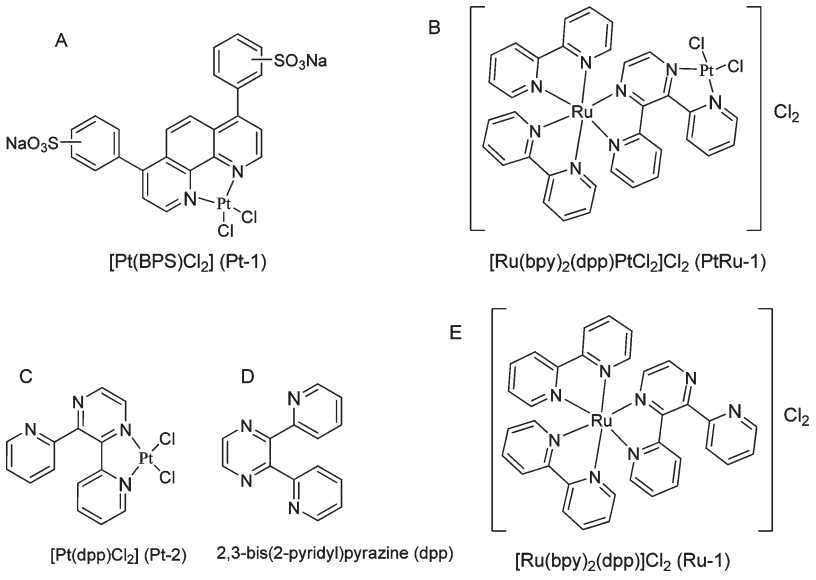

Figure 1. Chemical structures of the compounds used in this study.

Computational Investigations of Aβ−PtRu-1 Complex

To ascertain whether the introduction of Ru^{II} as the second metal center would enhance the binding capability of the primary metal center containing Pt^{II}, we first employed quantum chemical calculations to evaluate the comparative binding energies of the monometallic complex $(BL)Pt^{II}Cl_2$ (where bridging ligand = BL = dpp) and the binuclear complex $[(bpy)_2Ru^{II}(dpp)Pt^{II}Cl_2]Cl_2$ using a polyaromatic bridging ligand, dpp, since this kind of polyaromatic ligand was found to be crucial for the Aβ inhibition by the Pt-containing complex (*31*). Since the $(L)Pt^{II}Cl_2$ complexes inhibited Aβ aggregation as well as the Cu^{II}-mediated redox chemistry during Aβ aggregation, we used the proposed Cu^{II} binding sites in Aβ such as the histidines (H6 and H13/H14) and the N-terminal residue (*32*−*34*) as potential Pt^{II} binding sites in computing binding affinities, as shown in eqs 1−4, with an emphasis to compare the difference between the mononuclear complex and the binuclear one.

$$[(dpp)Pt^{II}Cl_2] + 2His \leftrightarrow [(dpp)Pt^{II}(His)_2]^{2+} + 2Cl^- \quad (1)$$

$$[(dpp)Pt^{II}Cl_2] + \text{N-terminus} \leftrightarrow [(dpp)Pt^{II}(\text{N-terminus})]^{2+} + 2Cl^- \quad (2)$$

$$[(bpy)_2Ru^{II}(dpp)Pt^{II}Cl_2]^{2+} + 2His \leftrightarrow [(bpy)_2Ru^{II}(dpp)Pt^{II}(His)_2]^{4+} + 2Cl^- \quad (3)$$

$$[(bpy)_2Ru^{II}(dpp)Pt^{II}Cl_2]^{2+} + \text{N-terminus} \leftrightarrow [(bpy)_2Ru^{II}(dpp)Pt^{II}(\text{N-terminus})]^{4+} + 2Cl^- \quad (4)$$

The histidine residues were indeed the primary ligands for the Pt-containing inhibitors as shown by NMR experiments (*35*). Interestingly, as shown in Table 1 both binding energies and enthalpies derived from our computational calculations suggest that histidine residues are preferred over the N-terminal residue. Due to the much larger entropy loss for binding of two separated histidine residues in such model calculations (shown in Supplementary Figure S1, Supporting Information; exact quantum chemical modeling of histidine residues in full-length Aβ42 is beyond current computational capability), the binding free energies of reactions eqs 1−4 show a little more favorable binding of the N-terminal residue over histidine residues. Nevertheless, compared with the monometallic complex $[(dpp)Pt^{II}Cl_2]$, the binuclear complex $[(bpy)_2Ru^{II}(dpp)Pt^{II}Cl_2]^{2+}$ exhibits much higher binding affinities in terms of all energetic properties investigated here for both binding sites. These results suggest that the binuclear complex $[(bpy)_2Ru^{II}(dpp)Pt^{II}Cl_2]^{2+}$ may possess a better Aβ inhibition behavior.

The Bimetal Complex, PtRu-1 Inhibited Aβ42 Aggregation

In order to explore whether our designed compound, PtRu-1, showed inhibitory behavior on Aβ42 aggregation, we co-incubated Aβ42 with varying concentrations of PtRu-1 and the previously reported Pt-1 as a positive control in separate reactions and monitored the aggregation by thioflavin-T (ThT) fluorescence (Figure 2A, B). In agreement with previous reports (*36*, *37*), incubation of Aβ42 alone at 37 °C resulted in an increase in fluorescence, indicating fibril formation (Figure 2A). But in sharp contrast, the co-incubated mixture of Aβ42 with a 2-fold molar excess Pt-1 did not show a significant

DOI: 10.1021/cn100046m | ACS Chem. Neurosci. (2010), 1, 691–701

Table 1. Binding Energetic Properties of Pt-Containing Complexes

complex	reaction	ΔE (kcal/mol)	ΔH (kcal/mol)	ΔG (kcal/mol)	ΔS (kcal/(mol K))
Pt-1	1	−22.56	−19.29	−11.41	−26.45
	2	−13.95	−11.31	−12.74	4.80
PtRu-1	3	−369.13	−365.65	−356.85	−29.51
	4	−361.76	−358.85	−360.25	4.69

increase in ThT fluorescence. Even after 200 h of incubation, the intensity was less than 10% of that of the control, suggesting inhibition (Figure 2A). Decreases in Pt-1 concentrations to substoichiometric levels (0.004:1 and 0.02:1 molar ratios of Pt-1 to Aβ) showed only marginal effect on aggregation (Figure 2A,B). Equimolar and 2-fold molar excess of Pt-1 resulted in nearly 90% reduction in fluorescence intensities after 200 h. Similar incubations of our designed compound, PtRu-1, with Aβ42 also showed inhibition to an extent that was nearly identical to that of Pt-1 (Figure 2B). The incubation with equimolar or 2-fold molar excess of PtRu-1 resulted in 90% reduction in ThT plateau levels while lower stoichiometric ratios resulted in steady increase in ThT levels. Both compounds exhibited a sigmoidal dose−response curve (Figure 2C) and a preliminary analysis of IC_{50} yielded almost identical values of ~4 μM for both Pt-1 and PtRu-1. This value for inhibition is slightly higher than the reported value of 0.4 μM of IC_{50} value for Pt-1 towards the inhibition of Cu^{2+}-mediated hydrogen peroxide generation of Aβ42 (*1*).

Inhibition by PtRu-1 Does Not Generate Oligomeric Intermediates as Opposed to Pt-1

We then wanted to see whether the inhibition leads to the formation of low-molecular weight oligomeric intermediates. This is important to know because if the inhibition results in the formation of oligomers, it may increase the toxicity since soluble oligomers are widely believed to be the primary toxic agents along the aggregation pathway. Since these oligomers are commonly referred as "SDS-stable" owing to their stability toward dissociation during electrophoresis, we decided to explore the presence of Aβ oligomeric intermediates, if any, generated by PtRu-1 by means of SDS-PAGE/Western blotting. However, it may not be necessary for all oligomers to be SDS-stable. Similar to Figure 2, Aβ42 samples were incubated in the presence of 2-fold molar excess of PtRu-1 and Pt-1. In addition, to make a precise estimate of the role of Ru^{II} center, we incubated Aβ42 with other control samples such as, Pt-2 (Pt with bridging ligand alone), Ru-1 (Ru with bridging ligand alone), and dpp (bridging ligand without metals) as shown in Figure 1. After 200 h of incubation at 37 °C, aliquots of samples were electrophoresed and transferred to a nitrocellulose membrane by Western blotting, and the blots were developed using monoclonal antibodies Ab9, 6E10, and 4G8 (Figure 3). The antibodies Ab9 and 6E10 have Aβ1−16 sequence as their epitopes, while Aβ17−24 forms the epitope for 4G8 (*38*, *39*)(Covance Inc., NJ). Clearly,

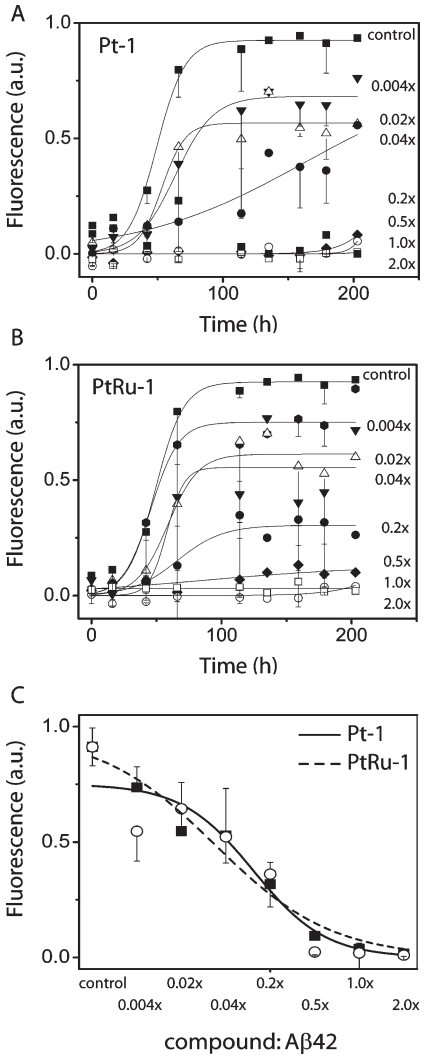

Figure 2. Inhibition of Aβ42 aggregation by Pt-1 and PtRu-1. (A, B) Dose−response curve obtained from ThT assay (average of two experiments). Aβ42 (25 μM) was incubated at 37 °C in buffer (20 mM Tris, 50 mM NaCl, pH 8.0) alone (■) or with varying concentration ratios of Pt-1 or PtRu-1/Aβ42: (A) 0.5 μM (▼), 1 μM (Δ), 5 μM (●), 12.5 μM (♦), 25 μM (○), 50 μM (□). Aliquots were diluted 15-fold into the buffer containing ThT. The solid lines are the fit of fluorescence to lag equation. (C) Curves showing fluorescence after 180 h of incubation of Aβ42 alone and with different concentrations of Pt-1 (○) and PtRu-1 (■). The data were fit using sigmoidal curve to obtain IC_{50} values.

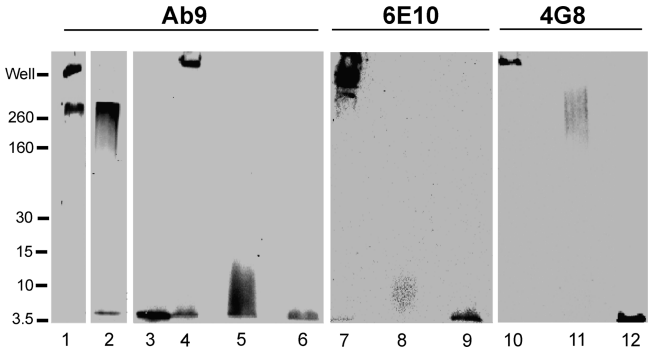

Figure 3. Immunoblots of Aβ42 inhibition by the designed compounds. The Aβ42 (25 μM) was incubated alone (control) or with 10-fold excess of compounds at 37 °C for 10 days. The samples (400 ng) were electrophoresed on a 12% polyacrylaminde gel followed by Western blotting and immunostaining using monoclonal antibodies Ab9, 6E10, and 4G8. Lanes 1−6, Ab9: Ru-1 (lane 1), Pt-2 (lane 2) ,and Aβ42 monomer (lane 3), control Aβ42 (lane 4), +Pt-1 (lane 5), +PtRu-1 (lane 6). Lanes 7−9, 6E10: control Aβ42 (lane 7), +Pt-1 (lane 8), +PtRu-1 (lane 9). Lanes 10−12, 4G8: control Aβ42 (lane 10), +Pt-1 (lane 11), and +PtRu-1 (lane 12).

the control Aβ42 sample in the absence of inhibitors showed the presence of aggregates larger than 200 kDa molecular weight with all three antibodies (lanes 4, 7, and 10, Figure 3), which is consistent with the formation of fibrils observed in ThT fluorescence data (Figure 2). The incubation of Pt-1 and PtRu-1 resulted in a significant inhibition of Aβ42 aggregation as observed by the absence of fibrils and the presence of monomeric bands (lanes 5 and 6, respectively), and more importantly, incubation with PtRu-1 did not indicate the presence of any oligomeric species when probed with Ab9 (lane 6, Figure 3). However, it was interesting to note that Pt-1 incubation generated a diffuse band in the ~7−10 kDa range corresponding to the molecular weight of dimer−trimer (2−3mer) (lane 5, Figure 3). We consistently, although with varying degrees of intensity, observed the diffuse 2−3mer band in all incubations with Pt-1 that was absent with PtRu-1. Probing the blot with 6E10 produced results that were similar to those from Ab9 (lanes 7−10, Figure 3). However, when the blot was probed with 4G8, we neither observed monomeric nor 2−3mer bands in co-incubations with Pt-1. Instead, a larger aggregate band ~100 kDa was observed that was absent in immunobots with Ab9 or 6E10. In addition, monomeric band was also absent, as opposed to PtRu-1 incubation (lanes 11 and 12). Furthermore, the immunoblots of the samples were probed with an "oligomer specific" antibody, A11 (*40*), to ascertain whether oligomers were present and specifically to see whether 2−3mers formed by Pt-1 could be detected. However, we failed to observe any bands in the blots, suggesting oligomeric species were absent in incubations containing both compounds (data not shown). These data may suggest two possibilities: (i) both Pt-1 and PtRu-1 are able to effectively inhibit Aβb42 aggregation and Pt-1 may be able generate or stabilize a 2−3mer form, although to a small extent compared to PtRu-1, and (ii) it is possible that both monomeric and oligomeric bands observed may arise due to the partial dissociation of diffuse aggregates upon addition of 1% SDS present in the sample buffer during electrophoresis. Therefore, caution is advised that SDS-PAGE must not be "overinterpreted". Nevertheless, immunoblotting with two antibodies with nonoverlapping epitopes of Aβ suggested that oligomers were formed in the presence of Pt-1 may have an assembly that is different from other aggregates. The control samples, Ru-1, Pt-2, and dpp (data not shown) failed to inhibit Aβ42 aggregation, which suggested that both Pt^{II} and Ru^{II} metal centers are essential for PtRu-1 to inhibit.

Fractionation of Aβ42 Aggregates Indicate Potential Differences between PtRu-1 and Pt-1

Next, we wanted to see whether the inhibition of Pt-1 indeed generated oligomeric intermediates as opposed to PtRu-1. Therefore, we fractionated Aβ42 incubations with 2-fold molar excess of PtRu-1 or Pt-1 incubated at 37 °C, using a Superdex-75 size exclusion chromatography (SEC) column after 400 h. The Aβ42 sample in buffer alone fractionated predominantly in the void volume with no indication of monomers present suggesting largely aggregated species in the sample (Figure 4A, B). This observation is consistent with the increased ThT fluorescence and >200 kDa band observed in SDS-PAGE gel (Figures 2 and 3 respectively). In a striking contrast, the fractionation of Aβ42 co-incubated with Pt-1 showed two peaks that were partially included in the column volume suggesting that they could be intermediates of aggregation (Figure 4C). However, the fractionation of Aβ42 co-incubated with PtRu-1 not only showed the absence of such intermediates, the sample also eluted in volumes that were more included than Aβ42 monomer itself (Figures 4A,D). The control samples did not show significant monomer retention in their elution profiles consistent with the SDS-PAGE data (data not shown). The metal complexes alone were fractioned close to the inclusion volume of the column, which is ~20 mL (fraction 40) (data not shown). These data suggest that the size of the aggregates inhibited with Pt-1 were larger than monomeric Aβ42 and those with PtRu-1 were smaller. It is possible that the binding of PtRu-1 may result in some structural changes leading to more "compact" Aβ monomer, in which case it can fractionate later in a SEC column. Nevertheless, it is clear from SEC fractionation that there is a significant difference between PtRu-1 and Pt-1 inhibitions of Aβ42 aggregation.

Mass Spectrometry Suggests Different Modes of Aβ−Inhibitor Interactions

The results from SEC fractionations encouraged us to explore whether we can detect the possible intermediates

DOI: 10.1021/cn100046m | *ACS Chem. Neurosci.* (2010), *1*, 691–701

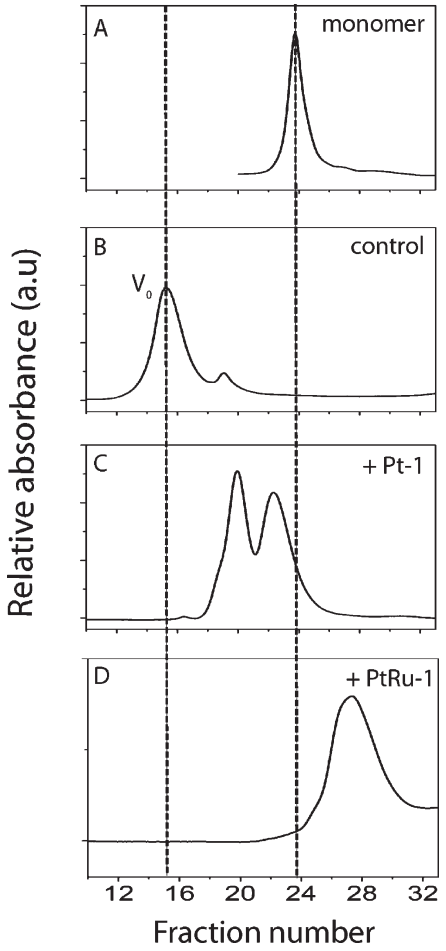

Figure 4. Size exclusion chromatography (SEC) analyses of Aβ42 inhibition. The Aβ42 samples incubated with 10-fold excess of Pt-1 or PtRu-1 were subjected to SEC fractionation after 18-days of incubation with a flow rate of 0.5 mL/min. (A) Aβ42 monomer control, (B) control Aβ42 in the absence of inhibitors, (C) Aβ42 with 2-fold excess of Pt-1, and (D) Aβ42 with 2-fold excess of PtRu-1. Aliquots of 250 μL samples were loaded on a Superdex-75 column, and the elutions were monitored at 215 nm. V_0 in the figure represents the void volume (7.5 mL) of the column. The inclusion volume of the column is ~20 mL (Fraction no. 40). This is data from one of the three experiments performed.

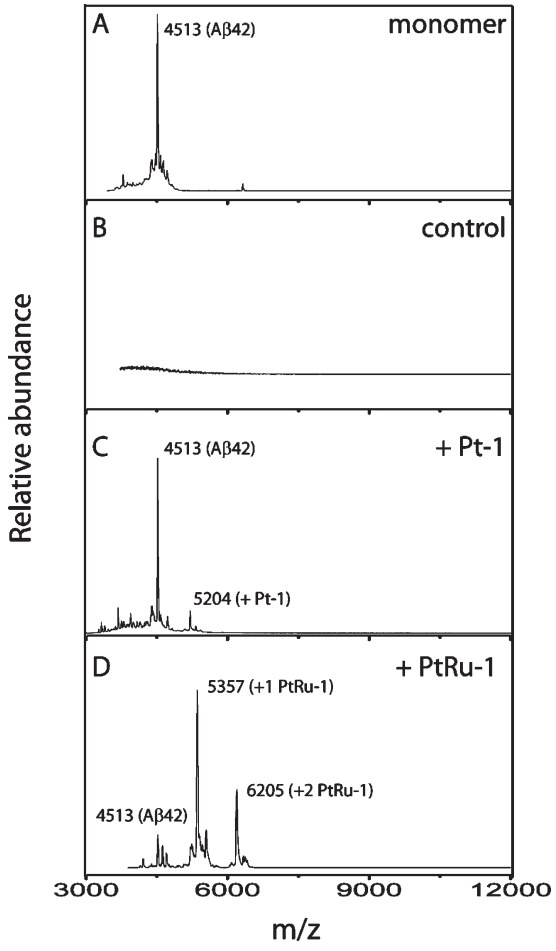

Figure 5. Mass spectrometry analysis of inhibition. Samples used for SEC in Figure 4 were analyzed by MALDI-ToF after 10-days of incubation. (A) Aβ42 monomer control, (B) Aβ42 alone in the absence of inhibitors, (C) Aβ42 with Pt-1, and (D) Aβ42 with PtRu-1. All the samples were mixed with sinapinic acid matrix to a final amount of 12 pmols.

with MALDI-ToF mass spectrometry. If what we observed as 2−3mers in SDS-PAGE gel is indeed real and not generated due to the dissociation during electrophoreses, we may be able to detect this species on MALDI (MW ~8−12 kDa). MALDI was performed in both linear and quadratic reflectron modes, and the instrument was calibrated with standards for both low (3−25 kDa; Protein Standard I) and high molecular weight (20−70 kDa; Protein Standard II) ranges. Aliquots of samples that were subjected to SEC (Figure 4) were analyzed on MALDI. The Pt-1 incubated sample showed an intense peak with m/z value of 4513 amu corresponding to monomeric Aβ42 and another less intense peak with a m/z value of 5204 amu that corresponded to Aβ42 bound to one molecule of Pt-1 as reported previously (*1*) (Figure 5C). However, we could not detect any peak above ~5300 amu, which we expected to observe for 2−3mer or any other oligomeric form. PtRu-1 indicated some unexpected peaks in MALDI. Besides a less intense monomeric peak, the sample indicated the presence of peaks with m/z values of 5357 and 6205 amu corresponding to one and two molecules of PtRu-1 bound to Aβ42 (Figure 5D). Although one cannot make quantitative assessments from MALDI data, we can say that a major amount of Aβ42 monomers are present in a form bound to PtRu-1. Based on the control Aβ42 sample spectrum, which showed no monomeric peak (Figure 5B) (consistent with the formation of fibrils), such a semiquantitative estimate is justified. The observation with PtRu-1 is in contrast to Pt-1, where the majority of Aβ42 monomers are not bound to Pt-1 (Figure 5C). Put together, the overall data suggests that the stoichiometry as well as the mode of binding to Aβ42 between the two compounds may

DOI: 10.1021/cn100046m | *ACS Chem. Neurosci.* (2010), *1*, 691–701

be different, consequently affecting their inhibitory capabilities.

Discussion

Data in this report collectively suggest that the bimetal complex, PtRu-1, inhibits Aβ42 aggregation nearly as effectively as the previously reported Pt-1 and form a fundamental basis for the development of multimetal complexes as inhibitors of Aβ aggregation. Also, PtRu-1displays distinct differences in binding and inhibition of Aβ42 compared with Pt-1. The data not only suggest a mechanism of PtRu-1 inhibition that possibly is different from that of Pt-1, but also shed insight into the details of Pt-1 inhibition that was not discussed in the previous report (*1*). First, Pt-1 inhibition generated intermediates observed in SEC fractionation that were clearly absent in PtRu-1 incubations. Our repeated attempts to characterize the intermediate fractions of Pt-1 (fractions 19 and 22; Figure 4C) by MALDI-ToF failed to indicate the presence of oligomers (data not shown). This may be due to poor desorption/flying of oligomeric ions from the matrix. To address this issue, we used different matrices such as α-cyano-hydroxy cinnamic acid (CHCA) and sinnapinic acid; however, we could not detect any oligomeric species. Nevertheless, this result was in stark contrast to PtRu-1, which did not show oligomeric intermediates in SEC, suggesting an extent of inhibition that is different from Pt-1. In fact, PtRu-1 incubations fractionated in later volumes than the monomer itself (Figure 4D). Furthermore, the MALDI mass spectrum of the unfractionated incubation of PtRu-1 clearly showed both one and two molecules of PtRu-1 bound to Aβ42 as opposed to one molecule of Pt-1 (Figure 4C,D). Also, the MALDI spectrum of fraction 28 indicated the presence of monomeric Aβ42 with two molecules of PtRu-1 bound (data not shown). It is clear from these data that there is more than one binding site for PtRu-1 in Aβ42 as opposed to one for Pt-1. As a consequence, PtRu-1 may alter the random coil conformation of monomeric Aβ42 to a more compactly folded form resulting in a smaller hydrodynamic radius observed by the delayed fractionation in SEC. Interestingly, both PtRu-1 and Pt-1 showed two peaks in SEC that may indicate two distinctly populated species, but we currently do not have any additional experimental evidence to claim so. It is also clear from the SDS-PAGE gels that the oligomeric intermediates generated in the presence of Pt-1 are not stable in high concentrations of SDS and dissociate during electrophoresis. Although we do not boil our samples prior to electrophoresis (because Aβ aggregates are well-known to dissociate (*37*, *41*), some aggregates may dissociate in high SDS concentrations, suggesting their instability. However, we did observe a diffuse banding pattern consistently in our gels between 8 and 12 kDa (2−3mer) with Pt-1. Nevertheless, it would be speculative to conclude whether these oligomers were pre-existent or generated during electrophoresis.

The precise measurement of binding energy, conformational changes, morphology, etc. still needs to be understood in order to gain molecular details of mechanism of inhibition, and we are currently in the process of doing so. Nevertheless, the "proof-of-concept" data presented here has shed insight into our rationale for developing structure-based multimetal complexes against Aβ aggregation. There are plenty of factors one can exploit in designing multimetal inhibitors, such as, choice of metal centers, which in turn can dictate the geometry and binding affinity around the binding site and choice of ligand to optimize both primary and secondary interactions with Aβ. In addition, organometallic compounds are unique in a way that one can design molecules to force the "randomly unstructured" Aβ monomer to bind and to convert the conformation to a potentially nonamyloidogenic conformation to effect inhibition, which is otherwise difficult. By doing so, one can develop inhibitors not only for Aβ but also for many other amyloidogenic proteins such as α-synuclein and prions, which are known to bind metals and are involved in pathogenesis of many neurodegenerative diseases.

Methods

Materials

Aβ42 was synthesized by the Peptide Synthesis Facility at the Mayo Clinic (Rochester, MN). MALDI-ToF mass spectrometry revealed >90% purity of both peptides. SDS, bovine serum albumin, and thioflavin T were procured from Sigma (St. Louis, MO). All other buffers and salts were obtained from VWR, Inc.

Syntheses of Organometallic Compounds

Commercial reagent grade chemicals and solvents, which were purchased from either Sigma-Aldrich or VWR Scientific, were used without further purification. *cis*-$[Pt(DMSO)_2Cl_2]$, $[Pt(BPS)Cl_2]$ (Pt-1), and $[Ru(bpy)_2(dpp)PtCl_2]^{2+}$ (PtRu-1) were prepared by previously reported procedures (*42*−*44*). The purity of the complexes was confirmed by ^{1}H NMR (Supplementary Table, Supporting Information).

Synthesis of $[Pt(dpp)Cl_2]$. This complex was synthesized as follows: $[Pt(DMSO)_2Cl_2]$ (0.116 g, 0.275 mmol) and methanol (30 mL) were added to a 100 mL round-bottom flask, followed by 2,3-bis(2-pyridyl) pyrazine (0.064 g, 0.273 mmol). The reaction mixture was stirred at room temperature for 24 h, then filtered. The residue was washed with methanol, followed by ether, and then air-dried. The filtrate was concentrated to a minimum volume by rotary evaporation; then the remaining product was precipitated with ether to yield a second crop of product. Combined yield = 0.1136 g (83%).

DOI: 10.1021/cn100046m | *ACS Chem. Neurosci.* (2010), *1*, 691–701

This compound was characterized by ^{1}H NMR (Supplementary Table, Supporting Information).

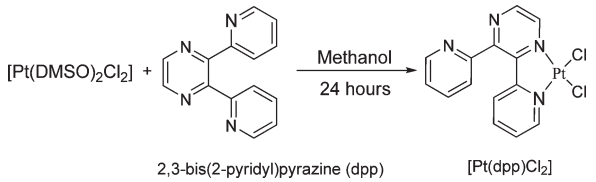

Computational Calculations

Structures of all species involved in reactions 1−4 were optimized using a hybrid Hartree−Fock and density functional theory method BHandHLYP (*45*, *46*) with a SDD (*47*) basis for metal elements and 6-31+G(d) basis for nonmetal elements, an approach similar to previous calculations of late transition metal complexes (*48*−*51*). For the bimetallic complexes, because the bpy ligands are not directly in contact with the Aβ residues that are coordinated to Pt, a 3-21G(d) basis was used for geometry optimization for efficiency. Enthalpies, entropies, and Gibbs free energies were also calculated at the same level of geometry optimization. However, the reported reaction electronic energies were evaluated at a higher level with a 6-311++G(2d,2p) basis for nonmetal elements and a SDD basis for metal elements, together with a PCM method (*52*−*56*) to account for solvent effects in the aqueous solutions. The energy differences of such high level calculations and corresponding low-level calculations were also added to the reaction enthalpies and reaction Gibbs free energies from direct geometry optimization and frequency calculations to yield the reported results in the text. All the calculations were carried out using the *Gaussian 03* program (*57*).

Polyacrylamide Gel Electrophoresis (PAGE) and Immunoblotting

Samples were dissolved in loading buffer (1× Laemmli buffer) containing 1% SDS, applied without heating to 12% acrylamide gels containing bis-Tris, and resolved in Laemmlli running buffer with 0.1% SDS. Dye-linked MW markers (Blue Plus2 Prestained Standards, Invitrogen) were run in parallel for calibration. Gels were electroblotted onto 0.45 μm Immobilon nitrocellulose membranes (BioTrace NT, Life Sciences Inc.). Blots were boiled in a microwave oven in PBS buffer for 2 min, blocked overnight with PBS buffer containing 5% nonfat dry milk and Tween 20, and probed (1.5−3 h) with 1:1000−1:2500 dilutions of monoclonal antibodies Ab9 or 6E10, which detect Aβ(1−16), or 4G8, whose epitope is Aβ-(17−24). Blots were then incubated with an anti-mouse horseradish peroxide (HRP) conjugate and developed with ECL reagent (Thermo Scientific Inc.).

MALDI-ToF Mass Spectrometry

MALDI-ToF mass data were collected on a Bruker Daltonics microflex (Bruker Inc.) using both linear and quadratic reflectron modes. The samples were mixed in equal volume with a saturated solution of absorbing matrix (sinnapinic acid or CHCA (10 mg/mL) in 50% ACN and 0.5% TFA), and 2 μL (10−12 pmol of Aβ42) was spotted on a MSP AnchorChip 600/96 A-H format (Bruker Daltonics). All the experiments were carried out at a laser intensity of 45% and detection gain ranging from 1.50 to 3.00 after calibration with both Protein Standards I and II (Bruker Daltonics) before each measurements.

Size Exclusion Chromatography (SEC)

Column preparation and use generally were described previously (*58*). In brief, samples (0.5−1.0 mL) were loaded onto a 1 × 30 cm^2 Superdex 75 HR 10/30 column (Amersham Pharmacia) attached to an AKTA FPLC system. The column was pre-equilibrated in 20 mM Tris-HCl (pH 8.0) at 25 °C and run at a flow rate of 0.5 mL/min. One minute fractions were collected.

Preparation of Aβ42 Monomers

Lyophilized stocks of Aβ42 were stored at −20 °C desiccated. The peptide was dissolved at 0.5−2.0 mM in 30 mM NaOH (*59*) 15 min prior to SEC on a Superdex 75 column. Peptide integrity after SEC was again confirmed by MALDI-ToF mass spectrometry. Monomeric Aβ42 was used within 2 days of SEC purification in all experiments. Concentrations of Aβ were determined by UV absorbance with a calculated extinction coefficient of 1450 cm^{-1} M^{-1} at 276 nm (www.expasy.org).

Aβ Aggregation Reactions

All reactions and measurements were made at room temperature unless otherwise noted. Reactions were initiated in siliconized eppendorf tubes by incubating appropriate concentrations of freshly purified Aβ monomer in buffer without agitation. Aggregation kinetic parameters were obtained by monitoring the reaction with ThT and fitting fluorescence data points to the sigmoidal curve in the following equation (*60*) using Origin 7.0.

$$F = \frac{a}{1 + e^{-[(t - t_{0.5})/b]}}$$

In this equation, t is time, a and b are fixed parameters, and $t_{0.5}$ is the time to reach half-maximal ThT fluorescence. Data points were unweighted. Lag times were equal to $t_{0.5} - 2b$ for each fitted curve.

Fluorescence Spectroscopy

ThT fluorescence measurements were performed as described previously (*58*, *61*). Briefly, the fluorescence was monitored in a microcuvette with a Cary Eclipse spectrometer (Varian Inc.) after 15-fold dilution of Aβ42 samples into 5 mM Tris-HCl (pH 8.0) containing 10 μM ThT. Continuous measurements were taken for 1 min with the excitation wavelength fixed at 450 nm, the emission fixed at 482 nm, and the excitation and emission slits set at 10 nm, and the average fluorescence value was determined. The fluorescence of solvent blanks was subtracted.

Supporting Information Available

Computational models of PtRu-1 binding to N-terminus of Aβ42 and ^{1}H NMR data for the ligand and complexes. This material is available free of charge via the Internet at http://pubs.acs.org.

Author Information

Corresponding Author

* To whom correspondence should be addressed. Tel: 601 266 6044. Fax: 601 266 6075. E-mail: vijay.rangachari@usm.edu.

Author Contributions

A.K. and V.R. generated all the biophysical data; J.F.O., N.L., and A.A.H. synthesized the complexes; R.L.K. and Y.Z. generated the computational data.

Funding Sources

The authors acknowledge the following funding agencies for their partial financial support: American Heart Association (Grant 0535185N) and Alzheimer's Association (Grant NIRG-09-132721) for V.R., NIH (Grant GM-085774) for Y.Z. and USM (A.A.H. and V.R.). The authors also acknowledge NSF for funding our ESI and MALDI-ToF mass spectrometers (Grant CHE 0639208).

Acknowledgment

The authors would like to acknowledge Lesley C. Lewis-Alleyne for her help in synthesis of [Pt(BPS)Cl_2]. We thank Mississippi Center for Supercomputing Research and USM Vislab for the generous use of the computing facilities. The authors also thank Mississippi Functional Genomics Network (MFGN) for allowing us to use their gel documentation facility.

Abbreviations

BPS, 4,7-diphenyl-1,10-phenanthroline disulfonic acid disodium salt; bpy, 2,2′-bipyridine; dpp, (2,3-bis(2-pyridyl)pyrazine.

References

1. Barnham, K. J., Kenche, V. B., Ciccotosto, G. D., Smith, D. P., Tew, D. J., Liu, X., Perez, K., Cranston, G. A., Johanssen, T. J., Volitakis, I., Bush, A. I., Masters, C. L., White, A. R., Smith, J. P., Cherny, R. A., and Cappai, R. (2008) Platinum-based inhibitors of amyloid-beta as therapeutic agents for Alzheimer's disease. *Proc. Natl. Acad. Sci. U.S.A. 105*, 6813–6818.

2. Brookmeyer, R., Gray, S., and Kawas, C. (1998) Projections of Alzheimer's disease in the United States and the public health impact of delaying disease onset. *Am. J. Public Health 88*, 1337–1342.

3. Hardy, J., and Selkoe, D. J. (2002) The amyloid hypothesis of Alzheimer's disease: Progress and problems on the road to therapeutics. *Science 297*, 353–356.

4. Lesne, S., Koh, M. T., Kotilinek, L., Kayed, R., Glabe, C. G., Yang, A., Gallagher, M., and Ashe, K. H. (2006) A specific amyloid-beta protein assembly in the brain impairs memory. *Nature 440*, 352–357.

5. Kawarabayashi, T., Shoji, M., Younkin, L. H., Wen-Lang, L., Dickson, D. W., Murakami, T., Matsubara, E., Abe, K., Ashe, K. H., and Younkin, S. G. (2004) Dimeric amyloid beta protein rapidly accumulates in lipid rafts followed by apolipoprotein E and phosphorylated tau accumulation in the Tg2576 mouse model of Alzheimer's disease. *J. Neurosci. 24*, 3801–3809.

6. Klein, W. L., Stine, W. B., Jr., and Teplow, D. B. (2004) Small assemblies of unmodified amyloid beta-protein are the proximate neurotoxin in Alzheimer's disease. *Neurobiol. Aging 25*, 569–580.

7. Kumita, J. R., Weston, C. J., Choo-Smith, L. P., Woolley, G. A., and Smart, O. S. (2003) Prevention of peptide fibril formation in an aqueous environment by mutation of a single residue to Aib. *Biochemistry 42*, 4492–4498.

8. Soto, C., Sigurdsson, E. M., Morelli, L., Kumar, R. A., Castano, E. M., and Frangione, B. (1998) Beta-sheet breaker peptides inhibit fibrillogenesis in a rat brain model of amyloidosis: implications for Alzheimer's therapy. *Nat. Med. 4*, 822–826.

9. Kokkoni, N., Stott, K., Amijee, H., Mason, J. M., and Doig, A. J. (2006) N-Methylated peptide inhibitors of β-amyloid aggregation and toxicity. Optimization of the inhibitor structure. *Biochemistry 45*, 9906–9918.

10. Rangachari, V, D. Z., Healy, B, Moore, B. D., Sonoda, L. K., Cusack, B, Maharvi, G. M., Fauq, A. H., and Rosenberry, T. L. (2009) Rationally designed dehydroalanine (ΔAla) containing peptides inhibit amyloid-beta(Aβ) peptide aggregation. *Biopolymers 91*, 456–465.

11. Yang, F., Lim, G. P., Begum, A. N., Ubeda, O. J., Simmons, M. R., Ambegaokar, S. S., Chen, P. P., Kayed, R., Glabe, C. G., Frautschy, S. A., and Cole, G. M. (2005) Curcumin inhibits formation of amyloid beta oligomers and fibrils, binds plaques, and reduces amyloid in vivo. *J. Biol. Chem. 280*, 5892–5901.

12. Ono, K., Hasegawa, K., Naiki, H., and Yamada, M. (2004) Anti-amyloidogenic activity of tannic acid and its activity to destabilize Alzheimer's beta-amyloid fibrils in vitro. *Biochim. Biophys. Acta 1690*, 193–202.

13. Ono, K., Hasegawa, K., Naiki, H., and Yamada, M. (2004) Curcumin has potent anti-amyloidogenic effects for Alzheimer's beta-amyloid fibrils in vitro. *J. Neurosci. Res. 75*, 742–750.

14. Bush, A. I. (2002) Metal complexing agents as therapies for Alzheimer's disease. *Neurobiol. Aging 23*, 1031–1038.

15. Bush, A. I. (2003) The metallobiology of Alzheimer's disease. *Trends Neurosci. 26*, 207–214.

16. Bush, A. I., Masters, C. L., and Tanzi, R. E. (2003) Copper, beta-amyloid, and Alzheimer's disease: Tapping a sensitive connection. *Proc. Natl. Acad. Sci. U.S.A. 100*, 11193–11194.

17. Garzon-Rodriguez, W., Yatsimirsky, A. K., and Glabe, C. G. (1999) Binding of Zn(II), Cu(II), and Fe(II) ions to Alzheimer's A beta peptide studied by fluorescence. *Bioorg. Med. Chem. Lett. 9*, 2243–2248.

18. Bush, A. I., Pettingell, W. H., Multhaup, G., d Paradis, M., Vonsattel, J. P., Gusella, J. F., Beyreuther, K., Masters, C. L., and Tanzi, R. E. (1994) Rapid induction of Alzheimer A beta amyloid formation by zinc. *Science 265*, 1464–1467.

19. Atwood, C. S., Scarpa, R. C., Huang, X., Moir, R. D., Jones, W. D., Fairlie, D. P., Tanzi, R. E., and Bush, A. I. (2000) Characterization of copper interactions with alzheimer amyloid beta peptides: identification of an attomolar-affinity copper binding site on amyloid beta1−42. *J. Neurochem. 75*, 1219–1233.

20. Karr, J. W., Akintoye, H., Kaupp, L. J., and Szalai, V. A. (2005) N-Terminal deletions modify the Cu2+ binding site in amyloid-beta. *Biochemistry 44*, 5478–5487.

DOI: 10.1021/cn100046m | *ACS Chem. Neurosci.* (2010), *1*, 691–701

21. Dong, J., Canfield, J. M., Mehta, A. K., Shokes, J. E., Tian, B., Childers, W. S., Simmons, J. A., Mao, Z., Scott, R. A., Warncke, K., and Lynn, D. G. (2007) Engineering metal ion coordination to regulate amyloid fibril assembly and toxicity. *Proc. Natl. Acad. Sci. U.S.A. 104*, 13313–13318.

22. Giaccone, G. (2000) Clinical perspectives on platinum resistance. *Drugs 59*, 9–17.

23. Cohen, S. M., and Lippard, S. J. (2001) Cisplatin: From DNA damage to cancer chemotherapy. *Prog. Nucleic Acid Res. Mol. Biol. 67*, 93–130.

24. Ho, Y.-P., Au-Yeung, S. C. F., and To, K. K. W. (2003) Platinum-based anticancer agents: Innovative design strategies and biological perspectives. *Med. Res. Rev. 23*, 633–655.

25. Fang, Z., Swavey, S., Holder, A., Winkel, B., and Brewer, K. J. (2002) DNA binding of mixed-metal supramolecular Ru, Pt complexes. *Inorg. Chem. Commun. 5*, 1078–1081.

26. Williams, R. L., Toft, H. N., Winkel, B., and Brewer, K. J. (2003) Synthesis, characterization, and DNA binding properties of a series of Ru, Pt mixed-metal complexes. *Inorg. Chem. 42*, 4394–4400.

27. Richter, M. M., and Brewer, K. J. (1992) Spectroscopic, electrochemical and spectroelectrochemical investigations of mixed-metal Os(II)/Ru(II) bimetallic complexes incorporating polypyridyl bridging ligands. *Inorg. Chem. 31*, 1594–1598.

28. Richter, M. M., and Brewer, K. J. (1993) Osmium/ruthenium trimetallics incorporating polyazine bridging ligands: Isovalent NIR absorbers with unique electrochemical behavior. *Inorg. Chem. 32*, 5762–5768.

29. Richter, M. M., and Brewer, K. J. (1993) Investigation of the spectroscopic, electrochemical and spectroelectrochemical properties of Os(II) complexes incorporating polyazine bridging ligands: Formation of the Os,Os and Os,Ru mixed-valence complexes. *Inorg. Chem. 32*, 2827–2834.

30. Carlson, D. L., Huchital, D. H., Mantilla, E. J., Sheardy, R. D., and Murphy, W. R., Jr. (1993) A new class of DNA metallobinders showing spectator ligand size selectivity: binding of ligand-bridged bimetallic complexes of ruthenium(II) to calf thymus DNA. *J. Am. Chem. Soc. 115*, 6424–6425.

31. Porat, Y., Abramowitz, A., and Gazit, E. (2006) Inhibition of amyloid fibril formation by polyphenols: structural similarity and aromatic interactions as a common inhibition mechanism. *Chem. Biol. Drug Des. 67*, 27–37.

32. Drew, S. C., Noble, C. J., Masters, C. L., Hanson, G. R., and Barnham, K. J. (2009) Pleomorphic copper coodination by Alzheimer's disease amyloid-β peptide. *J. Am. Chem. Soc. 131*, 1195–1207.

33. Dorlet, P., Gambarelli, S., Faller, P., and Hureau, C. (2009) Pluse EPR spectroscopy reveals the coordination sphere of copper(II) ions in the 1−16 amyloid-β peptide: A key role of the first two N-terminus residues. *Angew. Chem., Int. Ed. 48*, 9273–9276.

34. Hureau, C., Coppel, Y., Dorlet, P., Solari, P. L., Sayen, S., Guillon, E., Sabater, L., and Faller, P. (2009) Deprotonation of the Asp1-Ala2 peptide bond induces modification of the dynamic copper(II) environment in the amyloid-β peptide near physiological pH. *Angew. Chem., Int. Ed. 48*, 9522–9525.

35. Barnham, K. J., Kenche, V. B., Ciccotosto, G. D., Smith, D. P., Tew, D. J., Liu, X., Perez, K., Cranston, G. A., Johanssen, T. J., Volitakis, I., Bush, A. I., Masters, C. L., White, A. R., Smith, A. P., Cherny, R. A., and Cappai, R. (2008) Platinum-based inhibitors of amyloid-β as therapeutic agents for Alzheimer's Disease. *Proc. Natl. Acad. Sci. U. S. A. 105*, 6813–6818.

36. Naiki, H., Hasegawa, K., Yamaguchi, I., Nakamura, H., Gejyo, F., and Nakakuki, K. (1998) Apolipoprotein E and antioxidants have different mechanisms of inhibiting Alzheimer's β-amyloid fibril formation in vitro. *Biochemistry 37*, 17882–17889.

37. Rangachari, V., Moore, B. D., Reed, D. K., Bridges, A. W., Conboy, E., Hartigan, D., and Rosenberry, T. L. (2007) Amyloid-β(1−42) rapidly forms protofibrils and oligomers by distinct pathways in low concentrations of sodium dodecylsulfate. *Biochemistry 46*, 12451–12462.

38. Kukar, T., Murphy, M. P., Eriksen, J. L., Sagi, S. A., Weggen, S., Smith, T. E., Ladd, T., Khan, M. A., Kache, R., Beard, J., Dodson, M., Merit, S., Ozols, V. V., Anastasiadis, P. Z., Das, P., Fauq, A., Koo, E. H., and Golde, T. E. (2005) Diverse compounds mimic Alzheimer disease-causing mutations by augmenting Abeta42 production. *Nat. Med. 11*, 545–550.

39. Klyubin, I., Walsh, D. M., Lemere, C. A., Cullen, W. K., Shankar, G. M., Betts, V., Spooner, E. T., Jiang, L., Anwyl, R., Selkoe, D. J., and Rowan, M. J. (2005) Amyloid beta protein immunotherapy neutralizes Abeta oligomers that disrupt synaptic plasticity in vivo. *Nat. Med. 11*, 556–561.

40. Kayed, R., Head, E., Thompson, J. L., McIntire, T. M., Milton, S. C., Cotman, C. W., and Glabe, C. G. (2003) Common structure of soluble amyloid oligomers implies common mechanism of pathogenesis. *Science 300*, 486–489.

41. Moore, B. D., Rangachari, V., Tay, W. M., Milkovic, N. M., and Rosenberry, T. L. (2009) Biophysical analyses of synthetic amyloid-beta(1−42) aggregates before and after covalent cross-linking. Implications for deducing the structure of endogenous amyloid-beta oligomers. *Biochemistry 48*, 11796–11806.

42. De Pascali, S. A., Migoni, D., Papadia, P., Muscella, A., Marsigliante, S., Ciccarese, A., and Fanizzi, F. P. (2006) New water-soluble platinum(II) phenanthroline complexes tested as cisplatin analogues: First-time comparison of cytotoxic activity between analogous four- and five-coordinate species. *Dalton Trans.*5077–5087.

43. Price, J. H., Williamson, A. N., Schramm, R. F., and Wayland, B. B. (1972) Palladium(II) and platinum(II) alkyl sulfoxide complexes. Examples of sulfur-bonded, mixed sulfur- and oxygen-bonded, and totally oxygen-bonded complexes. *Inorg. Chem. 11*, 1280–1284.

44. Yam, V. W.-W., Lee, V. W.-M., and Cheung, K.-K. (1997) Synthesis, photophysics, electrochemistry, and reactivity of ruthenium(II) polypyridine complexes with organoplatinum(II) moieties. Crystal structure of $[Ru(bpy)_2(\mu\text{-}2,3\text{-}dpp)PdCl_2]^{2+}$. *Organometallics 16*, 2833–2841.

DOI: 10.1021/cn100046m | *ACS Chem. Neurosci.* (2010), *1*, 691–701

45. Becke, A. D. (1988) Density-functional exchange-energy approximation with correct asymptotic behavior. *Phys. Rev. A 38*, 3098–3100.

46. Lee, C., Yang, W., and Parr, R. G. (1988) Development of the Colle-Salvetti correlation-energy formula into a functional of the electron density. *Phys. Rev. B 37*, 785–789.

47. Leininger, T., Nicklass, A., Stoll, H., Dolg, M., and Schwerdtfeger, P. (1996) The accuracy of the pseudopotential approximation. 2. A comparison of various core sizes for indium pseudopotentials in calculations for spectroscopic constants of InH, InF, and InCl. *J. Chem. Phys. 105*, 1052–1059.

48. Zhang, Y., Guo, Z. J., and You, X. Z. (2001) Hydrolysis theory for cisplatin and its analogues based on density functional studies. *J. Am. Chem. Soc. 123*, 9378–9387.

49. Zhang, Y., Lewis, J. C., Bergman, R. G., Ellman, J. A., and Oldfield, E. (2006) NMR shifts, orbitals, and M center dot center dot center dot H-X bonding in d(8) square planar metal complexes. *Organometallics 25*, 3515–3519.

50. Balof, S. L., Yu, B., Lowe, A. B., Ling, Y., Zhang, Y., and Schanz, H. J. (2009) Ru-based olefin metathesis catalysts bearing pH-responsive N-heterocyclic carbene (NHC) ligands: Activity control via degree of protonation. *Eur. J. Inorg. Chem.*1717–1722.

51. Stevenson, S., Ling, Y., Coumbe, C. E., Mackey, M. A., Confait, B. S., Phillips, J. P., Dorn, H. C., and Zhang, Y. (2009) Preferential encapsulation and stability of La3N cluster in 80 atom cages: Experimental synthesis and computational investigation of La3N@C79N. *J. Am. Chem. Soc. 131*, 17780–17782.

52. Cossi, M., Barone, V., Cammi, R., and Tomasi, J. (1996) Ab initio study of solvated molecules: A new implementation of the polarizable continuum model. *Chem. Phys. Lett. 255*, 327–335.

53. Cossi, M., Barone, V., Mennucci, B., and Tomasi, J. (1998) Ab initio study of ionic solutions by a polarizable continuum dielectric model. *Chem. Phys. Lett. 286*, 253–260.

54. Cossi, M., Scalmani, G., Rega, N., and Barone, V. (2002) New developments in the polarizable continuum model for quantum mechanical and classical calculations on molecules in solution. *J. Chem. Phys. 117*, 43–54.

55. Cances, E., Mennucci, B., and Tomasi, J. (1997) A new integral equation formalism for the polarizable continuum model: Theoretical background and applications to isotropic and anisotropic dielectrics. *J. Chem. Phys. 107*, 3032–3041.

56. Mennucci, B., and Tomasi, J. (1997) Continuum solvation models: A new approach to the problem of solute's charge distribution and cavity boundaries. *J. Chem. Phys. 106*, 5151–5158.

57. Frisch, M. J., Trucks, G. W., Schlegel, H. B., Scuseria, G. E., Robb, M. A., Cheeseman, J. R., Montgomery, J. A., Jr., Vreven, T., Kudin, K. N., Burant, J. C., Millam, J. M., Iyengar, S. S., Tomasi, J., Barone, V., Mennucci, B., Cossi, M., Scalmani, G., Rega, N., Petersson, G. A., Nakatsuji, H., Hada, M., Ehara, M. Toyota, K., Fukuda, R., Hasegawa, J., Ishida, M., Nakajima, T., Honda, Y., Kitao, O., Nakai, H., Klene, M., Li, X., Knox, J. E., Hratchian, H. P., Cross, J. B., Bakken, V., Adamo, C., Jaramillo, J., Gomperts, R., Stratmann, R. E., Yazyev, O., Austin, A. J., Cammi, R., Pomelli, C., Ochterski, J. W., Ayala, P. Y., Morokuma, K., Voth, G. A., Salvador, P., Dannenberg, J. J., Zakrzewski, V. G., Dapprich, S., Daniels, A. D., Strain, M. C., Farkas, O., Malick, D. K., Rabuck, A. D., Raghavachari, K., Foresman, J. B., Ortiz, J. V., Cui, Q., Baboul, A. G., Clifford, S., Cioslowski, J., Stefanov, B. B., Liu, G., Liashenko, A., Piskorz, P., Komaromi, I., Martin, R. L., Fox, D. J., Keith, T., Al-Laham, M. A., Peng, C. Y., Nanayakkara, A., Challacombe, M., Gill, P. M. W., Johnson, B., Chen, W., Wong, M. W., Gonzalez, C., and Pople, J. A. (2004) *Gaussian 03*, Revision D.01, Gaussian, Inc., Wallingford, CT.

58. Nichols, M. R., Moss, M. A., Reed, D. K., Lin, W. L., Mukhopadhyay, R., Hoh, J. H., and Rosenberry, T. L. (2002) Growth of beta-amyloid(1−40) protofibrils by monomer elongation and lateral association. Characterization of distinct products by light scattering and atomic force microscopy. *Biochemistry 41*, 6115–6127.

59. Fezoui, Y., Hartley, D. M., Harper, J. D., Khurana, R., Walsh, D. M., Condron, M. M., Selkoe, D. J., Lansbury, P. T., Jr., Fink, A. L., and Teplow, D. B. (2000) An improved method of preparing the amyloid β-protein for fibrillogenesis and neurotoxicity experiments. *Amyloid 7*, 166–178.

60. Nielsen, L., Khurana, R., Coats, A., Frokjaer, S., Brange, J., Vyas, S., Uversky, V. N., and Fink, A. L. (2001) Effect of environmental factors on the kinetics of insulin fibril formation: Elucidation of the molecular mechanism. *Biochemistry*8397–8409.

61. LeVine, H., 3rd. (1993) Thioflavine T interaction with synthetic Alzheimer's disease beta-amyloid peptides: detection of amyloid aggregation in solution. *Protein Sci. 2*, 404–410.

DOI: 10.1021/cn100046m | *ACS Chem. Neurosci.* (2010), *1*, 691–701